[PROC. OF JSCE Structural Eng./Earthquake Eng. Vol. 2, No. 1 April 1985]

ANALYTICAL STUDY OF AN OVERHEAD FIGURE-8 TELECOMMUNICATION LINE UNDER A STEADY WIND

By Hiroki YAMAGUCHI, Yoshio YAMAWAKI**, Yozo FUJINO*** and Manabu ITO*****

The aeroelastic behavior of the overhead telecommunication line of figure-8 section is studied analytically in order to investigate the wind-induced galloping motion of the line. The governing equations of the telecommunication line are firstly derived taking account of its torsional displacement. Numerical analyses are also made on the wind-induced static deformation, the linear free oscillation under wind load and the dynamic response in a steady wind. The results of numerical analyses explain well the experimental fact seen in the wind tunnel test reported in Refs. 1)~4) and it is found that the galloping of the figure-8 telecommunication line can be simulated to some degree using the present analysis.

1. INTRODUCTION

The telecommunication line which consists of a telecommunication cable and a suspending steel cable with lashing wires has a particular geometric configuration of figure-8 section. It has been reported that wind-induced galloping motion of this telecommunication line frequently occurred under wind and caused serious operating problems. The authors have made a wind tunnel study and also some theoretical considerations on the galloping oscillations of the figure-8 telecommunication line[1)~4)]. Those studies revealed the fundamental characteristics of the galloping phenomena of the telecommunication line.

The objectives of this study are to analytically estimate static and dynamic behavior of the telecommunication line under a steady wind and to consider the galloping oscillations in more detail. Analysis of mono-cable equilibrium and stability in a steady wind has been made using the finite element method[5)]. However, since the telecommunication line consists of two cables and torsional displacement was found to play an important role in the phenomena[1)], the formulation and results in Ref. 5) are not directly applicable to this problem.

In the present paper, the governing equations of the telecommunication line are firstly derived taking account of its torsional displacement as well as its geometrical nonlinearity. Using these nonlinear equations, wind-induced static deformations, which are the fundamental cause of galloping[1)], are secondly calculated. Thirdly linear free oscillations about the wind-induced static configuration are solved by the complex eigenvalue analysis and lastly nonlinear aerodynamic responses of the telecommunication line

* Member of JSCE, Dr. Eng., Asst. Professor of Foundation Eng., Saitama University (Shimo-ohkubo 255, Urawa, Saitama)
** Member of JSCE, M. Eng., Agency of Science and Technology (Formerly Graduate Student, Univ. of Tokyo)
*** Member of JSCE, Ph. D., Assoc. Professor of Civil Eng., University of Tokyo
**** Member of JSCE, Dr. Eng., Prof. of Civil Eng., University of Tokyo

under a steady wind are simulated.

2. ANALYTICAL MODEL AND COORDINATE SYSTEMS

The telecommunication line consists of a structural cable and a telecommunication cable as shown in Fig. 1. The telecommunication cable is attached to the structural cable and its stiffness is considered to be negligible. The Bernoulli-Euler hypothesis is employed and St. Venant's torsion is considered for the structural cable.

The locus of the centroid of the structural cable at time t, as is also shown in Fig. 1, is a smooth curve line which is determined by a right-handed Cartesian coordinate system x^1, x^2, x^3 in the space. The curvilinear coordinate s is taken along the real length of the curve line at time t. The state variables of cable are hence represented by the two independent parameters s and t. Therefore the position vector $\boldsymbol{r}$ of the structural cable can be written in the form :

$$\boldsymbol{r}(s,\ t)=[x^1(s,\ t)\quad x^2(s,\ t)\quad x^3(s,\ t)][\boldsymbol{i}_1\quad \boldsymbol{i}_2\quad \boldsymbol{i}_3]^T \cdots (1)$$

in which $\{\boldsymbol{i}_1,\ \boldsymbol{i}_2,\ \boldsymbol{i}_3\}$ are the orthonormal base vectors in the $\{x^1,\ x^2,\ x^3\}$ space.

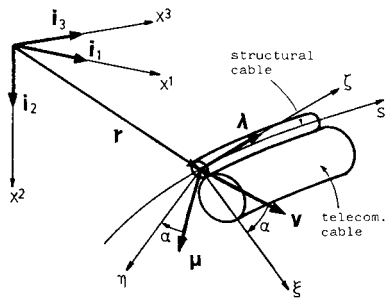

Fig. 1 Telecommunication line and coordinates.

In Fig. 1, λ, μ and ν denote the three unit vectors in the tangential, principal-normal and bi-normal directions on the curve, respectively; these vectors are defined as[6]

$$\lambda=\frac{\partial \boldsymbol{r}}{\partial s},\quad \mu=\frac{1}{\varkappa}\frac{\partial \lambda}{\partial s},\quad \nu=-\frac{1}{\tau}\left(\frac{\partial \mu}{\partial s}+\varkappa\lambda\right) \cdots (2\cdot a,\ b,\ c)$$

in which $\varkappa$, τ are the curvature and torsion of the curve, respectively. Substitution of Eq. (1) into Eqs. (2·a~c) yields

$$[\nu\quad \mu\quad \lambda]^T=[T_s][\boldsymbol{i}_1\quad \boldsymbol{i}_2\quad \boldsymbol{i}_3]^T \cdots (3\cdot a)$$

in which

$$[T_s]=\begin{bmatrix} \frac{1}{\varkappa}\left(\frac{\partial^2 x^2}{\partial s^2}\frac{\partial x^3}{\partial s}-\frac{\partial x^2}{\partial s}\frac{\partial^2 x^3}{\partial s^2}\right) & \frac{1}{\varkappa}\left(\frac{\partial^2 x^3}{\partial s^2}\frac{\partial x^1}{\partial s}-\frac{\partial x^3}{\partial s}\frac{\partial^2 x^1}{\partial s^2}\right) & \frac{1}{\varkappa}\left(\frac{\partial^2 x^1}{\partial s^2}\frac{\partial x^2}{\partial s}-\frac{\partial x^1}{\partial s}\frac{\partial^2 x^2}{\partial s^2}\right) \\ \frac{1}{\varkappa}\frac{\partial^2 x^1}{\partial s^2} & \frac{1}{\varkappa}\frac{\partial^2 x^2}{\partial s^2} & \frac{1}{\varkappa}\frac{\partial^2 x^3}{\partial s^2} \\ \frac{\partial x^1}{\partial s} & \frac{\partial x^2}{\partial s} & \frac{\partial x^3}{\partial s} \end{bmatrix} \cdots (3\cdot b)$$

The Lagrangian local coordinate system $\{\xi,\ \eta,\ \zeta\}$ fixed to the cable is also defined : ξ and η are two principal axes of the cross section while ζ is the axis along the tangential vector λ. The axis ξ contains the centroid of the telecommunication cable. The angle α is taken from the vector ν to the axis ξ and this parameter represents the twist angle of the cross section (Fig. 1). Then the following transformation holds

$$[\nu\quad \mu\quad \lambda]^T=[T_m][\boldsymbol{i}_\xi\quad \boldsymbol{i}_\eta\quad \boldsymbol{i}_\zeta]^T \cdots (4\cdot a)$$

in which

$$[T_m]=\begin{bmatrix} \cos\alpha & -\sin\alpha & 0 \\ \sin\alpha & \cos\alpha & 0 \\ 0 & 0 & 1 \end{bmatrix} \cdots (4\cdot b)$$

and $\{\boldsymbol{i}_\xi,\ \boldsymbol{i}_\eta,\ \boldsymbol{i}_\zeta\}$ are the base vectors in the coordinates $\{\xi,\ \eta,\ \zeta\}$.

3. BASIC EQUATIONS

(1) Equations of motion

The vector equations of motion of the telecommunication line can be readily derived by considering the

equilibrium of forces and moments acting on a differential segment of the cable shown in Fig. 2;

$$\frac{\partial \boldsymbol{F}}{\partial s}-\rho_1\frac{\partial^2 \boldsymbol{r}}{\partial t^2}-\rho_2\frac{\partial^2}{\partial t^2}(\boldsymbol{r}+\boldsymbol{d})+(\rho_1+\rho_2)g\boldsymbol{i}_2+\bar{\boldsymbol{p}}=\boldsymbol{0} \quad \cdots\cdots (5\cdot a)$$

$$\frac{\partial \boldsymbol{M}}{\partial s}+\lambda\times\boldsymbol{F}+\boldsymbol{d}\times\rho_2 g\boldsymbol{i}_2-m\frac{\partial^2\Theta}{\partial t^2}\lambda-\boldsymbol{d}\times\rho_2\frac{\partial^2}{\partial t^2}(\boldsymbol{r}+\boldsymbol{d})+\bar{\boldsymbol{m}}=\boldsymbol{0} \quad \cdots\cdots (5\cdot b)$$

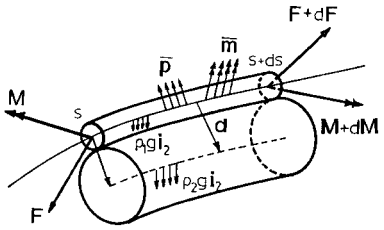

Fig. 2 Forces and moments acting on differential segment.

in which

$\boldsymbol{F}$: stress resultant force vector,

$\boldsymbol{M}$: stress resultant moment vector,

ρ_1, ρ_2 : masses per unit length of the structural cable and the attached cable, respectively,

$\boldsymbol{r}$: position vector of the structural cable,

$\boldsymbol{d}$: relative position vector of the attached cabre from the structural cable $(=d\times\boldsymbol{i}_\xi)$,

d : distance between the centroids of two cables,

$\bar{\boldsymbol{p}}$, $\bar{\boldsymbol{m}}$: vectors of external distributed force and moment,

m : torsional moment of inertia per unit length,

Θ : rotation angle of cross section.

Note that the third term of Eq. (5·b) accounts for a pendulum effect of the attached telecommunication cable mass.

(2) Stress resultant-deformation relations

The stress resultant force vector $\boldsymbol{F}$ may be decomposed into tension vector $\boldsymbol{T}$ and shear force vector $\boldsymbol{Q}$ while the stress resultant moment vector $\boldsymbol{M}$ is rotational moment vector $\boldsymbol{M}_T$ because of the negligible bending rigidity, i. e.

$$\boldsymbol{F}=\boldsymbol{T}+\boldsymbol{Q}=T\lambda+Q_\nu\nu+Q_\mu\mu,\quad \boldsymbol{M}=\boldsymbol{M}_T=M_T\lambda \quad \cdots\cdots (6\cdot a,\ b)$$

The tension T and the rotational moment M_T are related to the unit elongation ε and the rotation angle Θ respectively as

$$T=EA\varepsilon,\quad M_T=GJ\frac{\partial\Theta}{\partial s} \quad \cdots\cdots (7\cdot a,\ b)$$

where EA is the longitudinal rigidity and GJ is the torsional rigidity of the structural cable.

(3) Deformation-displacement relations

The elongation ε, curvature $\varkappa$ and torsion τ are defined as

$$(1+\varepsilon)^2=\left|\frac{\partial \boldsymbol{r}}{\partial s}\right|^2=\frac{\partial x^j}{\partial s}\cdot\frac{\partial x^j}{\partial s} \quad \cdots\cdots (8\cdot a)$$

$$\varkappa^2=\left|\frac{\partial\lambda}{\partial s}\right|^2=\left|\frac{\partial^2 \boldsymbol{r}}{\partial s^2}\right|^2=\frac{\partial^2 x^j}{\partial s^2}\cdot\frac{\partial^2 x^j}{\partial s^2} \quad \cdots\cdots (8\cdot b)$$

$$\tau=\frac{\partial\nu}{\partial s}\times\mu=\frac{1}{\varkappa^2}e_{ijk}\frac{\partial x^i}{\partial s}\cdot\frac{\partial^2 x^j}{\partial s^2}\cdot\frac{\partial^3 x^k}{\partial s^3} \quad \cdots\cdots (8\cdot c)$$

in which the index j is the dummy index and the symbol e_{ijk} denotes the permutation symbol.

Considering the differential rotation of unit vector $\boldsymbol{i}_\xi$ along s, the relation among the rotation angle Θ, the twist angle α and the torsion τ can be obtained as follows :

$$\frac{\partial\Theta}{\partial s}=\frac{\partial\alpha}{\partial s}+\tau \quad \cdots\cdots (9)$$

4. GOVERNING EQUATIONS OF TELECOMMUNICATION LINE

Substituting Eqs. (1) and (6·a) into Eq. (5·a) and using the transformation given by Eqs. (3) and (4), the equations of transverse motion in the $\boldsymbol{i}_1$, $\boldsymbol{i}_2$ and $\boldsymbol{i}_3$ directions can be derived as

$$\frac{\partial}{\partial s}\left(\frac{Q_\nu}{\varkappa}e_{ijk}\frac{\partial^2 x^j}{\partial s^2}\frac{\partial x^k}{\partial s}+\frac{Q_\mu}{\varkappa}\frac{\partial^2 x^i}{\partial s^2}+T\frac{\partial x^i}{\partial s}\right)-(\rho_1+\rho_2)\frac{\partial^2 x^i}{\partial t^2}+(\rho_1+\rho_2)g\delta_{i2}+\overline{p}^i=0 \qquad i=1,\ 2,\ 3 \quad \cdots\cdots (10)$$

in which $\overline{p}^i$ is the component of external force vector $\overline{\boldsymbol{p}}$ and the symbol δ_{ij} is the Kronecker delta. The inertia force caused by the torsion was neglected in Eq. (10).

Similarly, the equation of torsional motion (Eq. (11)) and the shear force-moment relations (Eq. (12)) are obtained from Eq. (5·b).

$$\frac{\partial M_T}{\partial s}-m\frac{\partial^2\Theta}{\partial t^2}+\rho_2 d\left(g\delta_{i2}-\frac{\partial^2 x^i}{\partial t^2}\right)\left(-\frac{\sin\alpha}{\varkappa}e_{ijk}\frac{\partial^2 x^j}{\partial s^2}\frac{\partial x^k}{\partial s}+\frac{\cos\alpha}{\varkappa}\frac{\partial^2 x^i}{\partial s^2}\right)+\overline{m}_T=0 \cdots\cdots (11)$$

$$Q_\nu=-\varkappa M_T+\rho_2 g d\cos\alpha\frac{\partial x^2}{\partial s}-\overline{m}_\mu,\quad Q_\mu=\rho_2 g d\sin\alpha\frac{\partial x^2}{\partial s}+\overline{m}_\nu \cdots\cdots (12\cdot a,\ b)$$

in which $\overline{m}_\nu$, $\overline{m}_\mu$, $\overline{m}_T$ are three components of the external moment vector $\overline{\boldsymbol{m}}$;

$$\overline{\boldsymbol{m}}=\overline{m}_\nu\boldsymbol{\nu}+\overline{m}_\mu\boldsymbol{\mu}+\overline{m}_T\boldsymbol{\lambda} \cdots\cdots (13)$$

The moments in ν and μ directions caused by the inertia force were neglected in Eqs. (12·a) and (12·b).

The governing equations of telecommunication line, i.e. Eqs. (10), (11) and (12) are nonlinear equations in displacements x^1, x^2, x^3, Θ and α. Considering that the angle α is represented by other displacements in Eq. (9), the unknown variables are only x^1, x^2, x^3 and Θ.

5. STATIC DEFORMATIONS DUE TO WIND FORCES

(1) Wind forces

The steady wind forces, drag D, lift L and moment M on the figure-8 section have been experimentally measured[2] and are expressed as

$$D=\frac{1}{2}\rho_0 U^2(2d)C_D \cdots\cdots (14\cdot a)$$

$$L=\frac{1}{2}\rho_0 U^2(2d)C_L \cdots\cdots (14\cdot b)$$

$$M=\frac{1}{2}\rho_0 U^2(2d)^2 C_M \cdots\cdots (14\cdot c)$$

where ρ_0 is the air density; U is the wind velocity; C_D, C_L and C_M are the steady wind force coefficient of drag, lift and moment obtained in the wind tunnel test (Fig. 3).

Consider that the wind direction is along the x^3-axis. The strip theory was accepted and the effect of the inclination of cable segment, caused by the initial sag and the deflection of cable, was neglected. The external forces and moments in Eqs. (10), (11) and (12) are hence given as

$$\overline{p}^1=0,\quad \overline{p}^2=-L,\quad \overline{p}^3=D \cdots\cdots (15\cdot a,\ b,\ c)$$

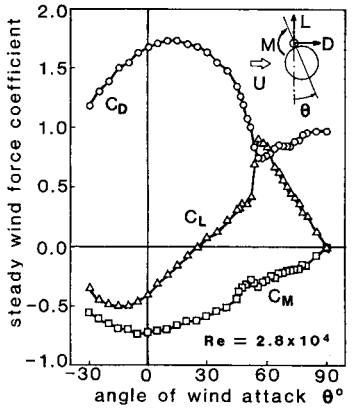

Fig. 3 C_D, C_L and C_M of figure-8 section $(d_2/d_1=5)$[2].

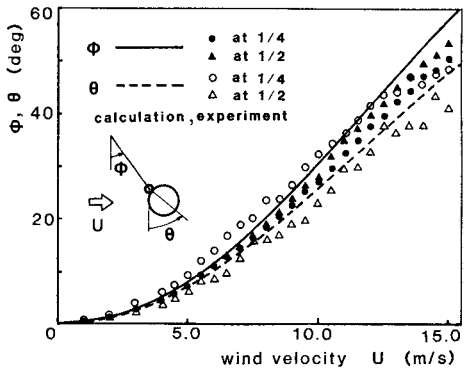

Fig. 4 Static deformation angles ϕ and θ vs. wind velocity U.

$\overline{m}_\nu=0,\ \overline{m}_\mu=0,\ \overline{m}_T=M$ ····· (16·a, b, c)

(2) Static analysis by incremental method

Considering the small displacements $(u,\ v,\ w,\ \theta,\ \gamma)$ from a static equilibrium state $(x_e,\ y_e,\ z_e,\ \Theta_e,\ \alpha_e)$, the three components of position vector of cable $(x^1,\ x^2,\ x^3)$ and the two torsional variables Θ and α are written as

$$x^1=x_e(s_e)+u(s_e,\ t),\quad x^2=y_e(s_e)+v(s_e,\ t),$$
$$x^3=z_e(s_e)+w(s_e,\ t) \cdots\cdots (17\cdot a,\ b,\ c)$$
$$\Theta=\Theta_e(s_e)+\theta(s_e,\ t),\quad \alpha=\alpha_e(s_e)+\gamma(s_e,\ t) \cdots\cdots (17\cdot d,\ e)$$

Table 1 Model parameters.

span length		ℓ	15 m
sag-to-span ratio		γ	0.03
structural cable	diameter	d_1	4.0 mm
	mass	ρ_1	25.0 g/m
	rigidity	EA	3.31×10^5N
		GJ	1.32×10^{-4}Nm
telecommunication cable	diameter	d_2	18.0 mm
	mass	ρ_2	375.0 g/m

where s_e is the curvilinear coordinate defined along the length of the static equilibrium curve line. Substituting Eqs. (17·a~e) into Eqs. (9), (10), (11) and (12) and neglecting the terms of higher orders, one can obtain the linearized equations of motion.

Taking account of the approximate shape of a catenary, the unknown independent-variables u, v, w and θ in those equations are assumed to be of the form (Appendix) :

$$u(s_e)=\sum_{i=1}^{N} o_i\left\{\sigma^{(2i+1)}-\left(\frac{1}{2}\right)^{2i}\sigma\right\},\quad v(s_e)=\sum_{i=1}^{N} p_i\left\{\sigma^{2i}-\left(\frac{1}{2}\right)^{2i}\right\},\quad w(s_e)=\sum_{i=1}^{N} q_i\left\{\sigma^{2i}-\left(\frac{1}{2}\right)^{2i}\right\} \cdots\cdots (18\cdot a,\ b,\ c)$$

$$\theta(s_e)=r_1+\sum_{i=2}^{M} r_i\left\{\frac{\sigma^{2i}}{2i}-\frac{\sigma^{(2i-2)}}{8i-8}\right\} \cdots\cdots (18\cdot d)$$

where σ is the curvilinear coordinate nondimensionalized by the initial cable length l^* :

$$\sigma=\frac{s_e}{l^*}-\frac{1}{2} \cdots\cdots (19)$$

Eqs. (18·a~d) are substituted into the linearized equations and Galerkin's method is applied. Neglecting inertia force terms, the coupled algebraic equations are finally obtained,

$$[K]\{q\}=\{f\},\quad \{q\}=[o_1\cdots,\ p_1\cdots,\ q_1\cdots,\ r_1\cdots]^T \cdots\cdots (20)$$

Giving a small increment of wind speed, that is, a small increment of the generalized external force vector $\{f\}$, one can compute the generalized displacement vector $\{q\}$ by Eq. (20) and then the increments of each displacement $(u,\ v,\ w,\ \theta)$ from Eqs. (18·a~d). Repeating this incremental technique, the static deformation of the telecommunication line under a certain wind speed can be calculated.

(3) Results and discussions

A numerical analysis is made for the single-span telecommunication line model which were used for the three-dimensional wind tunnel test in Ref. 1) and the model parameters are given in Table 1. The number of term N in Eqs. (18·a~c) is taken as 3 and M in Eq. (18·d) as 7.

Fig. 4 shows the calculated values of the inclination angle of the line (cable plane angle) ϕ and the angle of attack relative to the wind Θ. Their experimentally measured values[1] are also plotted for comparison in Fig. 4. One can see in Fig. 4 that the calculated static deformations fairly coincide with the experimental results.

6. LINEAR FREE OSCILLATION UNDER WIND LOAD

(1) Quasi-steady aerodynamic forces

The linear free oscillations of the line about the wind-induced static configuration are studied, considering a steady wind with speed U. The quasi-steady aerodynamic forces on the figure-8 line are

$$D=\frac{1}{2}\rho_0 U_T^2(2d)C_D,\quad L=\frac{1}{2}\rho_0 U_T^2(2d)C_L,\quad M=\frac{1}{2}\rho_0 U_T^2(2d)^2 C_M \cdots\cdots (21\cdot a,\ b,\ c)$$

where

$$U_T=\frac{U-\dot{w}}{\cos\beta^*},\quad \beta^*=\tan^{-1}\frac{\dot{v}}{U-\dot{w}} \cdots\cdots (22\cdot a,\ b)$$

in which a superposed dot represents a time derivative.

Accepting the strip theory, the non-zero external forces $\overline{p}^2$ and $\overline{p}^3$ can be written as:

$$\overline{p}^2=-L\cos\beta^*-D\sin\beta^*=\frac{1}{2}\rho_0 U^2(2d)C_{F2} \quad \cdots\cdots (23\cdot a)$$

$$\overline{p}^3=-L\sin\beta^*+D\cos\beta^*=\frac{1}{2}\rho_0 U^2(2d)C_{F3} \quad \cdots\cdots (23\cdot b)$$

where aerodynamic force coefficients C_{F2} and C_{F3} are defined by

$$C_{F2}=\left(\frac{U_r}{U}\right)^2(-\cos\beta^*\cdot C_L-\sin\beta^*\cdot C_D) \quad \cdots\cdots (24\cdot a)$$

$$C_{F3}=\left(\frac{U_r}{U}\right)^2(-\sin\beta^*\cdot C_L+\cos\beta\cdot {}^*C_D) \quad \cdots\cdots (24\cdot b)$$

Provided that the velocities of motion, $\dot{v}$ and $\dot{w}$ are small compared with the wind speed U, one can approximate β^* to

$$\beta^*\doteqdot\frac{\dot{v}}{U}\ll 1 \quad \cdots\cdots (25)$$

By this approximation, the non-zero external forces $\overline{p}^2$ and $\overline{p}^3$ and moment $\overline{m}_T$ are written finally as

$$\overline{p}^2=\frac{1}{2}\rho_0 U^2(2d)\left\{-\left(1-2\frac{\dot{w}}{U}\right)C_L-\left(\frac{\dot{v}}{U}\right)C_D\right\} \quad \cdots\cdots (26\cdot a)$$

$$\overline{p}^3=\frac{1}{2}\rho_0 U^2(2d)\left\{-\left(\frac{\dot{v}}{U}\right)C_L+\left(1-2\frac{\dot{w}}{U}\right)C_D\right\} \quad \cdots\cdots (26\cdot b)$$

$$\overline{m}_T=\frac{1}{2}\rho_0 U^2(2d)^2\left(1-2\frac{\dot{w}}{U}\right)C_M \quad \cdots\cdots (26\cdot c)$$

(2) Computational procedure

Taking into account the geometric boundary condition of no restraint in torsional motion at both fixed ends, the following forms of free oscillation are assumed,

$$u(s_e,\ t)=\sum_{i=1}^{N} o_i(t)\sin\frac{i\pi s_e}{l^*},\quad v(s_e,\ t)=\sum_{i=1}^{N} p_i(t)\sin\frac{i\pi s_e}{l^*},\quad w(s_e,\ t)=\sum_{i=1}^{N} q_i(t)\sin\frac{i\pi s_e}{l^*},$$

$$\theta(s_e,\ t)=\sum_{i=1}^{M} r_i(t)\cos\frac{i\pi s_e}{l^*} \quad \cdots\cdots (27\cdot a,\ b,\ c,\ d)$$

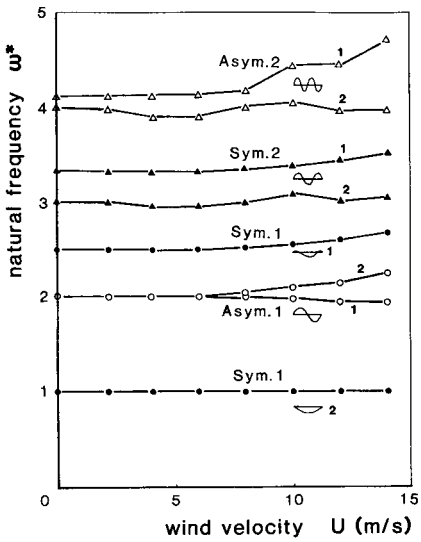

Fig. 5 Nondimensional natural frequency ω^* vs. wind velocity U.

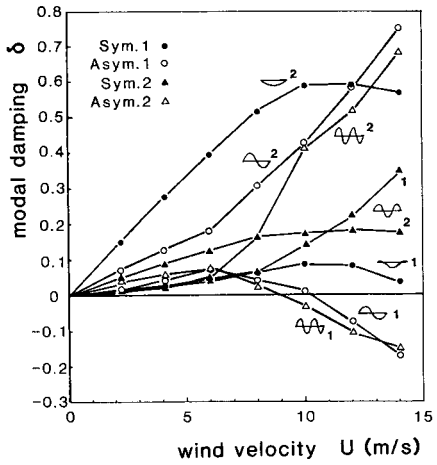

Fig. 6 Modal damping (logarithmic decrement) δ vs. wind velocity U.

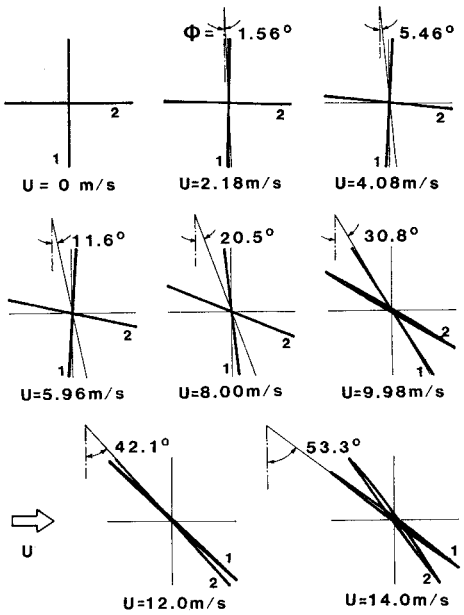

Fig. 7 Lissajous diagram of the first two symmetric modes at the mid-span.

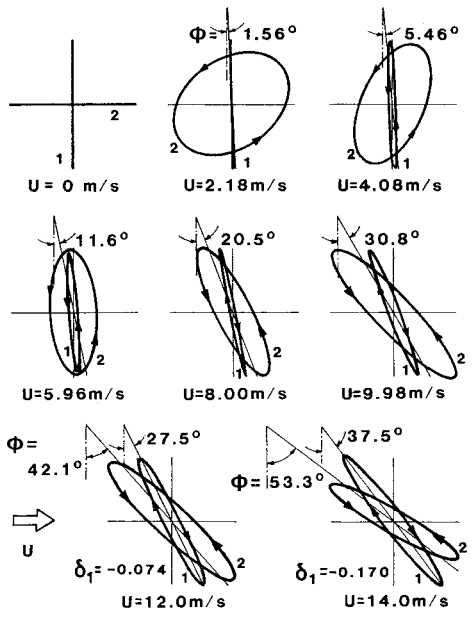

Fig. 8 Lissajous diagram of the first two asymmetric modes at the quarter-span.

in which o_i, p_i, q_i and r_i are the generalized coordinates.

By Galerkin's method, the linear ordinary differential equations for the generalized coordinates are obtained in the form

$$[M]\{\ddot{q}\}+[C_a]\{\dot{q}\}+[K]\{q\}=\{0\} \quad \cdots\cdots (28)$$

Applying the complex analysis, the natural frequencies, the associated modal damping coefficients and the modes can be calculated.

(3) Results and discussions

The complex eigenvalue analysis was carried out for the static deformed telecommunication line under various values of the wind speed : 0, 2.18, 4.08, 5.96, 8.00, 9.98, 12.0 and 14.0 m/s. Note that the numbers of term N' and M' in Eqs. (27·a~d) are taken as 5 and 20, respectively.

The natural frequencies ω^*, which are nondimensionalized with respect to the fundamental frequency of a tight string at $U=0$ m/s, are presented in Fig. 5 and the modal damping (logarithmic decrement) δ in Fig. 6. There are two kinds of natural oscillations which have the same or similar mode shape. In the case of still-air condition, these two kinds of oscillations are in-plane and out-of-plane motions. Small characters 1 and 2 for each mode in Figs. 5 and 6 distinguish between these motions and indicate the in-plane and out-of-plane motion at $U=0$ m/s, respectively.

It can be seen from Fig. 5 that the netural frequencies change slightly as the wind speed changes. This is because the restoring force is partly dependent on the aerodynamic forces. On the other hand, the modal damping coefficients change drastically as the wind speed changes (Fig. 6). The modal logarithmic decrements of the asymmetric first and second modes turn from positive to negative at about 10 m/s, indicating that the galloping of the telecommunication cable can occur in the asymmetric modes at this wind speed level. This result agrees with the experimental fact[1].

Although under still-air condition the linear free oscillation of cable is either in-plane motion or out-of-plane motion[7], in the case of steady wind action the principal directions of the free oscillations are in different planes which are not mutually perpendicular. The directions of motions calculated by the complex eigenvalue analysis are shown in Figs. 7 and 8 ; the Lissajous diagrams of the first two symmetric

modes at the mid-span in the vertical plane are presented in Fig. 7 while those of the first asymmetric modes at the quarter-span are in Fig. 8. The small characters 1 and 2 in Figs. 7 and 8 correspond to those in Figs. 5 and 6. These figures suggest that two kinds of the modes are not clearly identified as in-plane and out-of-plane motions. Furthermore, at $U=12.0$ m/s, it can be seen from Fig. 8 that one of the first asymmetric modes which has a negative modal damping coefficient oscillates in the direction inclined 27.5° from vertical direction. This angle 27.5° is smaller than the inclination angle of the line 42.1° calculated in 5. (3). Instead, it is very close to the angle of the self-excited motion in a small amplitude range measured at the wind tunnel test[1].

It should be noted that these natural symmetric and asymmetric modes are coupled with torsional motion as also verified by the experimental fact.

7. NONLINEAR AERODYNAMIC RESPONSES

(1) Analytical procedure

Should x^1, x^2, x^3, Θ and α be composed of the static equilibrium position (x_e, y_e, z_e, Θ_e, α_e) at the wind speed, where the galloping oscillation can occur, and dynamic displacements (u, v, w, θ, γ) from the position. In this section, however, the dynamic displacements are finite and the equations of motion are nonlinear.

It is convenient to assume expansions for the solutions of nonlinear equations in terms of linear normal mode in the form

$$[u \quad v \quad w \quad \theta]^T=\sum_i q_i(t)[\phi_{ui} \quad \phi_{vi} \quad \phi_{wi} \quad \phi_{\theta i}]^T \cdots\cdots (29)$$

in which $[\phi_{ui}\cdots\cdots\phi_{\theta i}]$ are the linear natural i-th modes calculated from the undamped system by the modal analysis.

Using Galerkin's method, one obtains the nonlinear ordinary differential equations for the generalized displacement vector $\{q\}$;

$$[M]\{\ddot{q}\}+[C_a(q,\ \dot{q})]\{\dot{q}\}+[K(q,\ \dot{q})]\{q\}=\{0\} \cdots\cdots (30)$$

Including modal structural damping, Eq. (30) becomes

$$[M]\{\ddot{q}\}+[M][\overline{\ }2h_i\omega_i^*\underline{\ }]\{\dot{q}\}+[C_a(q,\ \dot{q})]\{\dot{q}\}+[K(q,\ \dot{q})]\{q\}=\{0\} \cdots\cdots (31)$$

where h_i is the structural damping of the i-th mode.

The time history of the telecommunication line can be computed by the linear acceleration method. The adopted modes for the solution in Eq. (29) were only the first two asymmetric modes and a small initial velocity was imposed in the direction of largest aerodynamic exciting force of the first asymmetric mode.

(2) Results and discussions

Fig. 9 shows the calculated time-history responses of v, w and θ at the quarter span and the locus of motion in the vertical plane at $U=12.0$ m/s. The corresponding growth process of the galloping oscillation

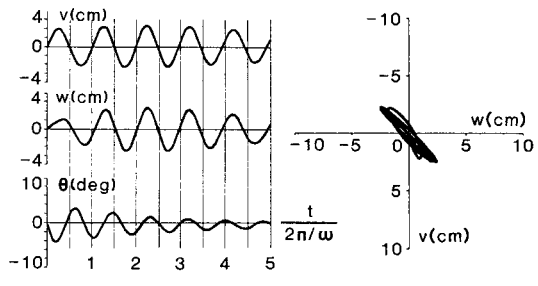

Fig. 9 Time-history response and locus of motion ($U=12.0$ m/s).

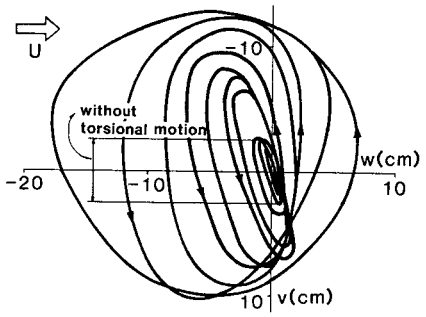

Fig. 10 Growth process of galloping motion in the wind tunnel test[1] ($U=11.5$ m/s).

in the wind tunnel test[1] is also presented in Fig. 10. In the experiment, it is reported that the galloping motion stays almost in a plane without torsional motion for a small amplitude range and that, after occurrence of torsional motion, the amplitudes increase rapidly into an elliptical locus with large torsional motion[1].

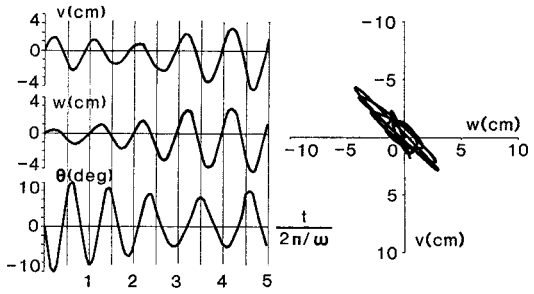

Fig. 11 Time-history response and locus of motion (U=14.0 m/s).

Comparing Fig. 9 with Fig. 10, the present calculation well simulates the self-excited motion in the small amplitude range. However, the significant torsional motion does not occur and the oscillation does not grow to the large amplitude motion. In the case of U=14.0 m/s (Fig. 11), the elliptical locus of the steady-state motion can not be simulated either, while the self-excited oscillation grows up with relatively large torsional motion. It is because the assumed solution for the torsional motion, that is only the torsional motions coupled with the asymmetric flexural modes, was insufficient to describe the large amplitude oscillation. It can be said from these results that the torsional response plays an important role in the growth of figure-8 telecommunication line.

8. CONCLUDING REMARKS

The aeroelastic behavior of the figure-8 telecommunication aerial line was studied analytically; the governing equations of the telecommunication line were derived taking account of its torsional displacement and numerical analyses were made on the wind-induced static deformation, the linear free oscillation about the wind-induced static configuration and the nonlinear aerodynamic response of the telecommunication line in a steady wind. Results of this study lead to the following brief conclusions :

(1) The calculated static deformations of the figure-8 telecommunication line under a steady wind fairly coincide with the experimental results.

(2) The natural mode shapes of the telecommunication line under wind load are not clearly identified as in-plane and out-of-plane motions.

(3) As the wind speed changes, the natural frequencies of the telecommunication line under wind load change slightly, but the modal damping coefficients change drastically. The modal logarithmic decrements, only for the asymmetric modes, turn from positive to negative at a certain wind speed level and this result is consistent with the experimental fact.

(4) The direction of the calculated first asymmetric mode at that wind speed is very close to the measured angle of the galloping motion in a small amplitude range.

(5) It is found that the present analysis is effective in the prediction of the galloping of the figure-8 telecommunication line. However, a nonlinear time-history response analysis proposed needs a further refinement in order to simulate the growth process of the galloping motion.

APPENDIX——ASSUMED SOLUTION FOR THE ROTATION ANGLE

The boundary condition of no restraint in rotation at both fixed ends is adopted. That is,

$$\frac{\partial\theta}{\partial\sigma}=0 \quad \text{at} \quad \sigma=\pm\frac{1}{2} \qquad \text{(A·1)}$$

Considering that the wind-induced static deformation of the rotation angle θ is symmetric along the span, the first derivative of θ with respect to σ is assumed to be of the form :

$$\frac{\partial\theta}{\partial\sigma}=\sum_{i=2}^{M} r_i\sigma^{2i-3}\left(\sigma^2-\frac{1}{4}\right) \qquad \text{(A·2)}$$

Integrating Eq. (A·2), one can obtain the assumed solution of Eq. (18·d) for θ.

ACKNOWLEDGMENT

Financial support by the Construction Technology Development Center, Nippon Telegram and Telephone Authority and the Ministry of Education, Science and Culture, Japan under Grant-in-Aid for Scientific Research is gratefully acknowledged.

REFERENCES

1) Ito, M., Fujino, Y. and Yamaguchi, H. : Wind Tunnel Study on Galloping Oscillations of Suspended Figure-8 Telecommunication Cables, Proc. of JSCE, Structural Eng./Earthquake Eng., Vol. 2, No. 1, April, 1985.
2) Tsuruta, I. : Aeroelastic Instability Oscillations of Suspended Figure-8 Telecommunication Cables, Master's Thesis, Dept. of Civil Eng., Univ. of Tokyo, 1983 (in Japanese).
3) Fukasawa, H. : Aeroelastic Behavior of Suspended Telecommunication Cables, Graduation Thesis, Dept. of Foundation Eng., Saitama Univ., 1984 (in Japanese).
4) Nomura, K. : Experimental and Analytical Study on Wind-Induced Oscillations of Figure-8 Suspended Cables, Graduation Thesis, Dept. of Civil Eng., Univ. of Tokyo, 1984 (in Japanese).
5) Russel, J. J., Morgan, J. D. and Henghold, W. M. : Cable Equilibrium and Stability in a Steady Wind, Proc. of ASCE, Vol. 104, No. ST 2, pp. 301~311, Feb., 1978.
6) Sokolnikoff, I. S. : TENSOR ANALYSIS, 2nd Edition, John Wiley & Sons, Inc., 1964.
7) Yamaguchi, H. and Ito, M. : Linear Theory of Free Vibrations of an Inclined Cable in Three Dimensions, Proc. of JSCE, Vol. 286, pp. 29~36, June, 1979 (in Japanese).

(Received September 25 1984)